Reprint from

Metal Forming Plasticity

IUTAM Symposium Tutzing/Germany
August 28 - September 3, 1978

Editor H. Lippmann

Springer-Verlag
Berlin · Heidelberg · New York

On the Prediction of Necking in Anisotropic Sheets

J.L. BASSANI
Dept. of Mechanical Engineering
Massachusetts Inst. of Technology
Cambridge, Mass. USA 02139

J.W. HUTCHINSON
Division of Applied Sciences
Harvard University
Cambridge, Mass. USA 02138

K.W. NEALE
Faculté des sciences appliquées
Université de Sherbrooke
Sherbrooke, Qué. CANADA J1K 2R1

Summary

Thin sheets with transversely isotropic material properties are studied, and we examine the effects of anisotropy on necking as predicted by various constitutive laws [1-3] which have been proposed for such metals. Both flow theory and deformation theory versions of the respective constitutive laws are considered. The results for both plasticity theories indicate that the necking strains and forming limit curves are strongly dependent on the *shape* of the anisotropic yield surface.

Introduction

A major difficulty which arises in the analysis of necking failures in thin sheets concerns the choice of an appropriate constitutive law to be incorporated in the analysis, since the predicted critical strains are often strongly dependent on the form of constitutive equation employed. For example, the use of the simplest finite-strain flow theory of plasticity leads to some questionable results for isotropic sheet materials [4]. In particular, for sheets subjected to in-plane biaxial stretching (where both principal strains are positive) this simple flow theory produces unrealistic "forming limit curves" and predicts that the critical strain for necking is exceptionally sensitive to small geometric imperfections. Furthermore, it indicates that a local necking

mode of bifurcation cannot occur in a perfect sheet. On the other hand, the predicted trends obtained using a finite-strain deformation theory appear to be in much better agreement with reported experimental data. Even when the respective plasticity theories are extended to include the influence of material strain-rate-dependence, deformation theory seems to give a better qualitative agreement with the trends of experiments than does simple flow theory [5].

A realistic analysis of necking in sheet metals must eventually account for the effects of anisotropy. In this study we restrict attention to sheets with *transversely isotropic* material properties. Constitutive laws based on the yield criteria proposed by Hill [1,2] and Bassani [3] for such metals are used to determine the influence of anisotropy on necking. Since the detailed shapes of the yield surfaces depend on the parameters in the yield functions, it becomes possible to examine whether slight changes in the *shape* of the assumed anisotropic yield surface are important. We shall see that this is the case, and that the predicted necking or "limit" strains are very sensitive to the shape of the yield surface.

Yield Functions for Transversely Isotropic Sheets

To date, the most widely known constitutive law for transversely isotropic materials is based on a yield criterion due to Hill [1], who proposed the following yield function for plane stress

$$(\sigma_1+\sigma_2)^2 + (1+2R)\ (\sigma_1-\sigma_2)^2 = 2(1+R)\sigma_u^2 \qquad (1)$$

Here, σ_1 and σ_2 are the principal stresses in the plane of the sheet ($\sigma_3=0$), the 3-axis is the axis of transverse isotropy, σ_u is the yield stress in uniaxial tension and R is the corresponding ratio of in-plane transverse plastic strain-increment to the thickness plastic strain-increment. As a consequence of (1), the ratio of yield stress in equi-biaxial tension ($\sigma_1=\sigma_2=\sigma_b$) to yield

stress in uniaxial tension becomes

$$\frac{\sigma_b}{\sigma_u} = \left(\frac{1+R}{2}\right)^{1/2} \qquad (2)$$

implying that the σ_b/σ_u ratio lies on the same side of unity as does R. This trend is not always confirmed experimentally and leads to what has been termed as "anomalous behaviour" by Woodthorpe and Pearce [6].

Hill [2] has since modified his original criterion (1) and suggested the following three-parameter yield function

$$|\sigma_1+\sigma_2|^n + (1+2R)\,|\sigma_1-\sigma_2|^n = 2(1+R)\sigma_u^n \qquad (3)$$

for which the σ_b/σ_u ratio now becomes

$$\frac{\sigma_b}{\sigma_u} = \frac{1}{2}\,[2(1+R)]^{1/n} \qquad (4)$$

The "anomalous behaviour" can clearly be incorporated here, and this theory obviously reduces to Hill's original function (1) for n=2. Parmar and Mellor [7] have recently employed Hill's new yield criterion (3) together with the flow theory of plasticity to predict the limit strains occurring in in-plane stretching. They report that, for the test results given in [8] for aluminum, an improved correlation between theory and experiment is obtained when Hill's original criterion (1) is replaced by (3).

In a recent study [3], Bassani has compared several families of yield functions for polycrystals, including (3), with those calculated from a Bishop-Hill procedure. Ideal textures giving rise to transversely isotropic properties that could be expected for typical sheet metals were considered. Hill's new criterion (3) did not prove to be entirely adequate for predicting details of the yield loci obtained from the Bishop-Hill calculations. The following four-parameter family of yield functions

$$|\sigma_1+\sigma_2|^n + \frac{n}{m}(1+2R)\sigma_u^{n-m}|\sigma_1-\sigma_2|^m = [1+\frac{n}{m}(1+2R)]\sigma_u^n \qquad (5)$$

was then introduced by Bassani in [3], and it was found to be sufficiently flexible to accurately approximate yielding for a wide range of transversely isotropic materials. Convexity of the yield function requires that $n,m \geq 1$, and for $n=m$ (5) reduces to (3). Bassani's criterion (5) gives the following relationship for the equi-biaxial to uni-axial yield stress ratio

$$\frac{\sigma_b}{\sigma_u} = \frac{1}{2}[1 + \frac{n}{m}(1+2R)]^{1/n} \qquad (6)$$

which again can account for the anomalous behaviour. A typical comparison between a yield locus calculated by the Bishop-Hill procedure (solid curve) and the phenomenological yield loci obtained from (3) and (5) (broken lines) is shown in Fig. 1.* For this case R=2.7 and the ratio σ_b/σ_u=1.02.

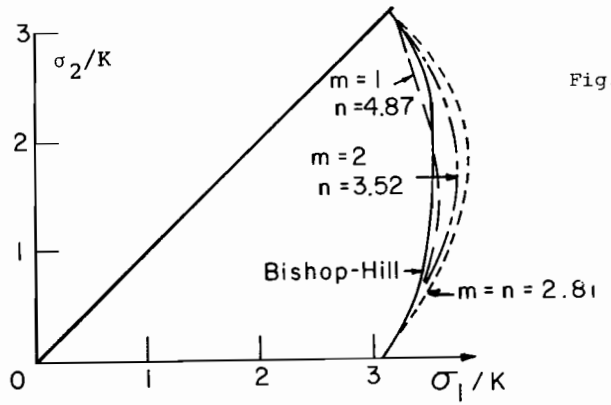

Fig. 1: Yield loci for [321] ideal texture, R=2.7

In the subsequent analysis the material is assumed to be rigid-plastic. Bassani's yield function is employed, with $\sigma_1 \geq \sigma_2$, so the expression for effective stress σ_e is given by the implicit relation

$$\sigma_e[1+\frac{n}{m}(1+2R)]^{1/n} = [(\sigma_1+\sigma_2)^n + \frac{n}{m}(1+2R)\sigma_e^{n-m}(\sigma_1-\sigma_2)^m]^{1/n} \qquad (7)$$

---

* This figure is taken from [3] (Fig. 7).

The effective stress is homogeneous of degree one in the stress components. Using σ_e as the flow potential leads to the following flow theory constitutive law

$$d\varepsilon_i = d\lambda \frac{\partial \sigma_e}{\partial \sigma_i} \qquad i=1,2 \qquad (8)$$

From the condition that the plastic work satisfies $dW = \sigma_i d\varepsilon_i = \sigma_e d\varepsilon_e$, where $d\varepsilon_e$ is the effective strain-increment, it follows that $d\lambda = d\varepsilon_e$. The constitutive equation (8) then takes the form

$$\frac{d\varepsilon_1}{(\sigma_1+\sigma_2)^{n-1}+(1+2R)(\sigma_1-\sigma_2)^{m-1}\sigma_e^{n-m}} = \frac{d\varepsilon_2}{(\sigma_1+\sigma_2)^{n-1}-(1+2R)(\sigma_1-\sigma_2)^{m-1}\sigma_e^{n-m}} = \frac{-d\varepsilon_3}{2(\sigma_1+\sigma_2)^{n-1}} = \frac{d\varepsilon_e}{[1+\frac{n}{m}(1+2R)]\sigma_e^{n-1}+(1-\frac{n}{m})(1+2R)(\sigma_1-\sigma_2)^m\sigma_e^{n-m-1}} \qquad (9)$$

Since σ_1 and σ_2 are principal stresses, the corresponding finite-strain deformation theory constitutive law [4] is obtained by simply replacing $d\varepsilon_i$, $d\varepsilon_e$ in (9) by their total (logarithmic) values ε_i and ε_e.

M-K Analysis for Imperfect Sheets

The present analysis, for determining limit strains in biaxially-stretched sheets, is along the lines of that introduced by Marciniak and Kuczynski ("M-K") [9]. We consider a sheet (Fig. 2) subjected to proportional straining $(\varepsilon_1,\varepsilon_2)$ or stressing (σ_1,σ_2) along its edges such that

$$\frac{\varepsilon_2}{\varepsilon_1} = \rho = \text{const} \quad , \quad \frac{\sigma_2}{\sigma_1} = \alpha = \text{const} \qquad (10)$$

where the fixed values of strain ratio ρ will be taken from ρ=0 (plane strain) to ρ=1 (equi-biaxial tension). The sheet initially has a nonuniformity in the form of a narrow band perpendicular to

the major principal strain ε_1. The thickness at the minimum section in the band is denoted by $h^B(t)$, with an initial value $h^B(0)$; whereas the region outside the band, referred to as the "uniform" section, has thickness h(t) with an initial value h(0). The initial geometric nonuniformity is defined as

$$\xi = \frac{h(0)-h^B(0)}{h(0)} \geq 0 \tag{11}$$

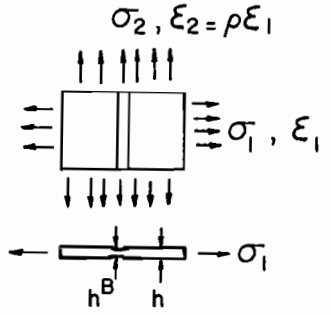

Fig. 2: Sheet geometry and loading

Throughout the analysis a superscript B will denote quantities along the minimum band section, and the absence of this symbol will refer to quantities in the uniform region. As discussed in [10], it is tacitly assumed in this M-K type analysis that the width-to-thickness ratio of the band is large.

According to the M-K simplification, the stress state over each cross-section is considered to be uniform; that is, the stress and strain components are quantities which are averaged through the thickness. The equilibrium condition across the band is simply

$$\sigma_1 h = \sigma_1^B h^B \tag{12}$$

We assume the relation between effective stress σ_e and the effective strain ε_e, obtained from a uniaxial true stress-natural strain curve, to be of the form

$$\sigma_e = K\varepsilon_e^N \tag{13}$$

This, together with (12) and the definitions

$$\varepsilon_3 = \ell n \frac{h}{h(0)} \quad , \quad \varepsilon_3^B = \ell n \frac{h^B}{h^B(0)} \tag{14}$$

leads to the following expression

$$\frac{\sigma_1}{\sigma_e} = (1-\xi) \frac{\sigma_1^B}{\sigma_e^B} \left(\frac{\varepsilon_e^B}{\varepsilon_e}\right)^N \exp(\varepsilon_3^B - \varepsilon_3) \tag{15}$$

The object of the subsequent analysis is to express all stress and strain quantities in (15) in terms of ε_e and ε_e^B. From the relationship between ε_e and ε_e^B we can calculate the development of the band and, in particular, determine the limit (maximum) strains attained in the uniform region of the sheet.

In the uniform section, where (10) holds, the expression (7) becomes

$$[(1+\alpha)\psi]^n + \frac{n}{m}(1+2R)\ [(1-\alpha)\psi]^m = 1 + \frac{n}{m}(1+2R) \tag{16}$$

in which $\psi = \sigma_1/\sigma_e = \text{const}$. The constitutive law (9), or its deformation theory equivalent, then gives

$$\rho = \frac{d\varepsilon_2}{d\varepsilon_1} = \frac{\varepsilon_2}{\varepsilon_1} = \frac{[(1+\alpha)\psi]^{n-1} - (1+2R)\ [(1-\alpha)\psi]^{m-1}}{[(1+\alpha)\psi]^{n-1} + (1+2R)\ [(1-\alpha)\psi]^{m-1}} \tag{17}$$

So given ρ we can solve (16) and (17) for α and ψ. From (9), (10) and the definition for ψ it follows that

$$\frac{d\varepsilon_2}{d\varepsilon_e} = \frac{\varepsilon_2}{\varepsilon_e} = \frac{[(1+\alpha)\psi]^{n-1} - (1+2R)\ [(1-\alpha)\psi]^{m-1}}{[1+\frac{n}{m}(1+2R)] + (1-\frac{n}{m})(1+2R)\ [(1-\alpha)\psi]^m} \equiv b \tag{18}$$

and

$$\frac{d\varepsilon_3}{d\varepsilon_e} = \frac{\varepsilon_3}{\varepsilon_e} = \frac{-2\,[(1+\alpha)\psi]^{n-1}}{[1+\frac{n}{m}(1+2R)] + (1-\frac{n}{m})(1+2R)\ [(1-\alpha)\psi]^m} \equiv -c \tag{19}$$

Again, both flow theory and deformation theory lead to the above results since proportional loading (b,c = const.) occurs in the uniform region.

For straining within the band, we introduce the following variables analogous to α and ψ

$$\alpha^B = \frac{\sigma_2^B}{\sigma_1^B} \quad , \quad \psi^B = \frac{\sigma_1^B}{\sigma_e^B} \tag{20}$$

which, in general, do not remain constant during deformation. Equation (7) becomes [c.f. (16)]

$$[(1+\alpha^B)\psi^B]^n + \frac{n}{m}(1+2R)[(1-\alpha^B)\psi^B]^m = 1+\frac{n}{m}(1+2R) \tag{21}$$

and using (19), (20) and the relations $\psi = \sigma_1/\sigma_e$, the equilibrium condition (15) can be written as

$$\frac{\psi}{\psi^B} = (1-\xi)\left(\frac{\varepsilon_e^B}{\varepsilon_e}\right)^N \exp(c\varepsilon_e + \varepsilon_3^B) \tag{22}$$

For flow theory, the expressions analogous to (18) and (19) are

$$\frac{d\varepsilon_2^B}{d\varepsilon_e^B} = \frac{[(1+\alpha^B)\psi^B]^{n-1} - (1+2R)[(1-\alpha^B)\psi^B]^{m-1}}{[1+\frac{n}{m}(1+2R)] + (1-\frac{n}{m})(1+2R)[(1-\alpha^B)\psi^B]^m} \tag{23}$$

and

$$\frac{d\varepsilon_3^B}{d\varepsilon_e^B} = \frac{-2[(1+\alpha^B)\psi^B]^{n-1}}{[1+\frac{n}{m}(1+2R)] + (1-\frac{n}{m})(1+2R)[(1-\alpha^B)\psi^B]^m} \tag{24}$$

The corresponding relations for deformation theory have $\varepsilon_2^B/\varepsilon_e^B$ and $\varepsilon_3^B/\varepsilon_e^B$ in place of $d\varepsilon_2^B/d\varepsilon_e^B$ and $d\varepsilon_3^B/d\varepsilon_e^B$ on the left-sides of (23) and (24).

When the compatibility requirement $d\varepsilon_2^B = d\varepsilon_2$ (or $\varepsilon_2^B = \varepsilon_2$) is used together with (18) and (23), the following expression is obtained

$$\frac{d\varepsilon_e^B}{d\varepsilon_e} = b\,\frac{[1+\frac{n}{m}(1+2R)] + (1-\frac{n}{m})(1+2R)[(1-\alpha^B)\psi^B]^m}{[(1+\alpha^B)\psi^B]^{n-1} - (1+2R)[(1-\alpha^B)\psi^B]^{m-1}} \tag{25}$$

This relation is valid for the flow theory case and, as previously, the corresponding deformation theory expression consists of substituting $\varepsilon_e^B/\varepsilon_e$ for $d\varepsilon_e^B/d\varepsilon_e$ in (25). For n=m, i.e., with Hill's new criterion (3), equations (21) to (25) reduce to those derived by Parmar and Mellor in [7]. They also reduce to the expressions given in [8] when n=m=2.

Flow theory results were obtained from a straightforward incremental solution of (24) and (25). This determined the band deformation ε_e^B in terms of the prescribed uniform deformation ε_e. In the numerical solution, the strain ratio ρ was initially specified, and (16) and (17) were solved for α and ψ using a Newton-Raphson technique. A similar iterative procedure was employed at each increment to solve (21) and (22) for α^B and ψ^B. On the other hand, the results of ε_e^B for given ε_e according to deformation theory were obtained from a direct numerical solution of (21), (22) together with the deformation theory relations corresponding to (24) and (25). In all solutions the maximum value of strain attained in the uniform part of the sheet was determined for prescribed values of ρ. We refer to this limiting value of uniform strain, where $d\varepsilon_e/d\varepsilon_e^B = 0$, as the "limit" strain or critical strain for localized necking as it represents the state where the deformation becomes concentrated in the band while the remainder of the sheet begins to unload.

Results and Discussion

The previous analysis was applied to generate numerical results for initial strain ratios varying from ρ=0 (plane strain) to ρ=1 (equi-biaxial tension). Theoretical limit strains are plotted in Figs. 3-6 as "forming limit curves", i.e., curves which illustrate the dependence of the limit strain ε_1^* on imposed strain ratio. In these figures, the solid and dashed curves refer to the deformation theory and flow theory predictions, respectively. Results

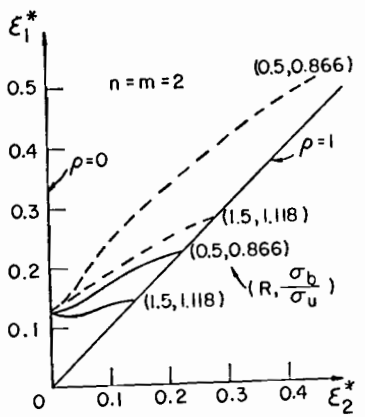

Fig. 3

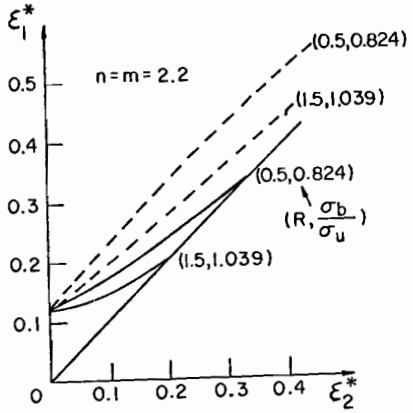

Fig. 4

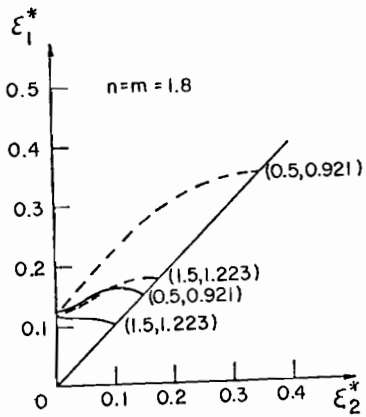

Fig. 5

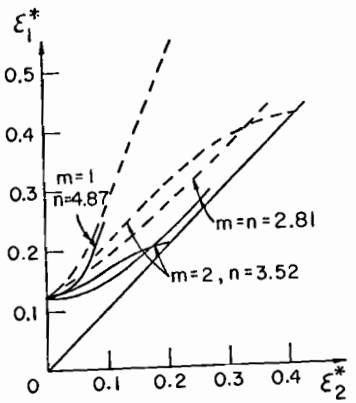

Fig. 6

Figs. 3-6:
Forming limit curves for N=0.20 and ξ=.02 (solid lines refer to deformation theory and dashed curves to flow theory).

are shown for a strain-hardening exponent N=0.20 and an initial imperfection ξ=0.02. The numbers in parentheses next to each curve in Figs. 3-5 denote the R-values and associated σ_b/σ_u ratios, respectively.

The results in Fig. 3 are obtained with Hill's original yield function (1), i.e., n=m=2, and the flow theory curves here are representative of previously given M-K analyses [7,8]. These curves rise much more steeply with increasing ρ than the corresponding deformation theory curves, especially as the R-value is decreased. Experimentally observed forming limit curves (e.g. [8]) do not appear to rise as rapidly as flow theory would predict, but seem to be more in line with the trends of deformation theory. It was apparently this discrepancy between the flow theory predictions and test data that prompted Parmar and Mellor [7] to seek a better correlation using Hill's new criterion (3) in their flow theory analysis.

In Figs. 4 and 5, results determined using Hill's new criterion (3) are shown with n=m=2.2 and 1.8, respectively. The shapes of the forming limit curves here are seen to be extremely sensitive to small changes in the n=m values. In particular, as we approach the equi-biaxial stretching condition (ρ=1) the limit strain for given R is reduced drastically as the σ_b/σ_u ratio is increased. The flow theory curve for n=m=1.8 (Fig. 5) and R=0.5 is identical to that given in [7] and, as mentioned previously, this trend is in better agreement with experiments than the corresponding curve in Fig. 3. Nevertheless, the experimental forming limit curve [8] for aluminum still tends to be much flatter than the flow theory prediction for n=m=1.8, and bears more resemblance to the theoretical deformation theory curve.

Bassani's yield function (5) was employed to compute the results shown in Fig. 6. An R-value = 2.7 and a fixed ratio σ_b/σ_u=1.02 were assumed for these calculations; and m,n were chosen to produce

the phenomenological yield surfaces of Fig. 1. In this way one could examine the effect of the *shape* of the yield surface on the predicted trends. It is clear from Fig. 6 that the forming limit curves are strongly dependent on the parameters m and n, that is on the details of the yield locus. This observation holds for both plasticity theories, despite the fact that the flow theory curves generally lie well above the deformation theory curves and predict much higher limit strains as $\rho \to 1$.

What seems to be particularly important is the shape of the yield surface near the equi-biaxial stress state. In Fig. 1 the yield locus for m=2, n=3.52 appears to best fit the results of the Bishop-Hill calculation at the equi-biaxial state ($\sigma_1=\sigma_2$), and it is for this case alone in Fig. 6 that we obtain "reasonable" forming limit curves. Although the choice m=1, n=4.87 gives perhaps the best overall approximation to the Bishop-Hill locus, it produces a poor fit near $\sigma_1=\sigma_2$ and leads to unrealistic forming limit curves. Furthermore, computational difficulties arise with m=1 because of the corner which exists in the yield surface at the equi-biaxial state. The forming limit curves in Fig. 6 for n=m=2.81 also seem somewhat unrealistic.

We finally note that the additional calculations were carried out for other values of m, n, R and σ_b/σ_u considered by Bassani in [3]. These cases examined corresponded to Figs. 6 and 9 of [3], where again m=2 gives a better approximation to the Bishop-Hill yield curve near the equi-biaxial state than m=1 or m=n. The trends and conclusions here are essentially the same as discussed above; namely, (i) flow theory generally predicts much higher limit strains than deformation theory as $\rho \to 1$, and (ii) the theoretical forming limit curves for both plasticity theories are strongly dependent on the detailed shapes of the anisotropic yield surfaces, especially on their shapes in the vicinity of the equi-biaxial stress state.

Acknowledgments

The work of J.L.B. and J.W.H. was supported in part by the National Science Foundation (Grant ENG 76-04019) and by the Division of Applied Sciences, Harvard University. The work of K.W.N. was supported by the National Research Council of Canada (Grant A-8584).

References

1 Hill, R.: The Mathematical Theory of Plasticity. Oxford University Press, London (1978).

2 Hill, R.: private communication (1976).

3 Bassani, J.L.: Yield characterization of metals with transversely isotropic plastic properties. Int. J. Mech. Sci. 19 (1977) 651-660.

4 Hutchinson, J.W.; Neale, K.W.: Sheet necking - II Time-independent behaviour. Proc. GM Symp. on Mechanics of Sheet Metal Forming. Plenum Press, New York (1978).

5 Hutchinson, J.W.; Neale, K.W.: Sheet necking - III Strain-rate effects. ibid.

6 Woodthorpe, J.; Pearce, R.: The anomalous behaviour of aluminum sheet under balanced biaxial tension. Int. J. Mech. Sci. 12 (1970) 341-347.

7 Parmar, A.; Mellor, P.B.: Predictions of limit strains in sheet metal using a more general yield criterion. Int. J. Mech. Sci. 20 (1970) 385-391.

8 Marciniak, Z.; Kuczynski, K.; Pokora, T.: Influence of the plastic properties of a material on the forming limit diagram for sheet metal in tension. Int. J. Mech. Sci. 15 (1973) 789-805.

9 Marciniak, Z.; Kuczynski, K.: Limit strains in the processes of stretch-forming sheet metal. Int. J. Mech. Sci. 9 (1976) 609-620.

10 Hutchinson, J.W.; Neale, K.W.; Needleman, A.: Sheet necking-I Validity of plane stress assumptions of the long-wavelength approximation. Proc. GM Symp. on Mechanics of Sheet Metal Forming. Plenum Press, New York, (1978).